

Electromagnetic low-energy constants in χ PT

C. Haefeli^{1,a}, M.A. Ivanov², M. Schmid³

¹ Departament de Física Teòrica, IFIC, Universitat de València – CSIC, Apt. Correus 22085, 46071 València, Spain

² Laboratory of Theoretical Physics, Joint Institute for Nuclear Research, 141980 Dubna (Moscow region), Russia

³ Institute for Theoretical Physics, University of Bern, Sidlerstr. 5, 3012 Bern, Switzerland

Received: 7 November 2007 /

Published online: 22 December 2007 – © Springer-Verlag / Società Italiana di Fisica 2007

Abstract. We investigate three-flavour chiral perturbation theory including virtual photons in the limit in which the strange quark mass is much larger than the external momenta and the up and down quark masses, and where the external fields are those of two-flavour chiral perturbation theory. In particular, we work out the strange quark mass dependence of the electromagnetic two-flavour low-energy constants C and k_i . We expect that these relations will be useful for a more precise determination of the electromagnetic low-energy constants.

PACS. 11.30.Rd; 12.39.Fe; 13.40.Dk; 13.40.Ks

1 Introduction

Chiral perturbation theory (χ PT) [1–3] is the effective theory of QCD at low energies. It relies on an effective Lagrangian whose coupling constants are the chiral low-energy constants (LECs). They are independent of the light quark masses and encode the influence of the heavy degrees of freedom that are not contained in the Lagrangian explicitly. For many phenomenological applications the predictivity of χ PT depends on realistic estimates of these LECs. An up-to-date account of our knowledge about the LECs can be found in the recent conference reports of Ecker [4] and Bijmans [5].

In this article we are concerned with the electromagnetic LECs of χ PT in the (natural parity) meson sector including virtual photons. In the following we abbreviate the effective theory with three flavours by χ PT₃ ^{γ} [6–8], and accordingly for two flavours by χ PT₂ ^{γ} [9–11]. Recently, quite some progress has been achieved estimating the NLO electromagnetic LECs in χ PT₃ ^{γ} [12–17], while little is known about the pertinent LECs in χ PT₂ ^{γ} , to the best of our knowledge. In such a situation the following strategy may be pursued [18–20]: if one limits the external momenta to values small compared to the kaon and eta mass and treats m_u and m_d as small in comparison to m_s ,

$$|p^2| \ll M_K^2 \quad m_u, m_d \ll m_s, \quad (1)$$

then the degrees of freedom of the kaons and the eta freeze. In this region one may work out relations among the LECs in χ PT₂ ^{γ} and χ PT₃ ^{γ} , which allow one to estimate the electromagnetic LECs in χ PT₂ ^{γ} through the know-

ledge of the ones in χ PT₃ ^{γ} . The purpose of the present article is to systematically provide *all* relations between the $O(e^2, e^2 p^2, e^4)$ LECs in χ PT₂ ^{γ} and χ PT₃ ^{γ} at one-loop order. The calculation is performed along the lines outlined in [21–23]. Briefly, the method consists in a non-trivial matching between the three-flavour versus the two-flavour generating functional of the effective theory.¹

We briefly comment on related work in the literature. Analogous relations between the two-flavour and the three-flavour LECs in the strong sector have been provided by Gasser and Leutwyler in [3]. Recently, we have worked out the same relations to the next higher order (at two loops) in the perturbative expansion [23]; see also [25, 26] for earlier contributions to the literature on such relations at two loops. Finally, analogous work was performed at one-loop accuracy in the baryonic sector in [27].

The remainder of the article is organised as follows. After settling on the notation in Sect. 2, we give some details on the derivation of the matching relations in Sect. 3. Section 4 contains a numerical analysis of the matching relations, leading to estimates of the electromagnetic NLO LECs in χ PT₂ ^{γ} .

2 Including virtual photons in χ PT

A general procedure to construct the effective theory with photons in the mesonic sector for three light flavours

¹ After we had performed the calculation of these matching relations, we were informed by Marc Knecht that the relations at $O(e^2)$ and $O(e^2 p^2)$ had also been derived by Nehme [24]. We agree with the relations given there.

^a e-mail: haefeli@itp.unibe.ch, haefeli@ific.uv.es

(χ PT₃ ^{γ}) has been proposed by Urech [6]. The two-flavour effective theory χ PT₂ ^{γ} may be constructed along the same lines [9–11]. We choose our notation following the nomenclature of the LECs introduced by Urech [6] for χ PT₃ ^{γ} , and by Knecht and Urech [9] for χ PT₂ ^{γ} .

The basic building block of the chiral Lagrangian is the Goldstone matrix field $u(\phi)$ which transforms under a chiral rotation $g = (g_L, g_R) \in \text{SU}(n) \times \text{SU}(n)$ as

$$u(\phi) \xrightarrow{g} u(\phi') = g_R u(\phi) h(g, \phi)^{-1} = h(g, \phi) u(\phi) g_L^{-1},$$

where h is called the compensator field. The mesonic Lagrangian then consists of operators X that either transform as

$$X \xrightarrow{g} h(g, \phi) X h(g, \phi)^{-1} \quad (2)$$

or remain invariant under chiral transformations. As a result, (products of) traces of products of chiral operators X are chiral invariant. The elementary building blocks of the effective Lagrangian that have the transformation property of (2) and furthermore contain the external vector v_μ , axial a_μ (both traceless), scalar s , and pseudoscalar p sources are given by

$$\begin{aligned} u_\mu &= i [u^\dagger (\partial_\mu - i r_\mu) u - u (\partial_\mu - i l_\mu) u^\dagger], \\ \chi_\pm &= u^\dagger \chi u^\dagger \pm u \chi^\dagger u, \end{aligned} \quad (3)$$

where

$$\begin{aligned} r_\mu &= v_\mu + a_\mu + Q_R A_\mu, \quad l_\mu = v_\mu - a_\mu + Q_L A_\mu, \\ \chi &= 2B_0(s + ip), \end{aligned} \quad (4)$$

with A_μ the photon field and $Q_{L,R}$ spurion sources with the transformation properties

$$Q_R \xrightarrow{g} g_R Q_R g_R^\dagger, \quad Q_L \xrightarrow{g} g_L Q_L g_L^\dagger.$$

They are also contained in the building blocks

$$q_R = u^\dagger Q_R u, \quad q_L = u Q_L u^\dagger, \quad (5)$$

which transform according to (2). Below, we will consider constant sources $Q_R = Q_L = Q$ only, and of phenomenological interest are the cases with two ($Q = Q_2$), as well as three light flavours ($Q = Q_3$),

$$Q_2 = \frac{e}{3} \text{diag}(2, -1), \quad Q_3 = \frac{e}{3} \text{diag}(2, -1, -1). \quad (6)$$

Note that Q_3 is traceless, while Q_2 is not. For three flavours the leading order Lagrangian reads in Euclidean space-time,

$$\begin{aligned} \mathcal{L}_2^{(3)} &= \frac{F_0^2}{4} \langle u \cdot u - \chi_+ \rangle - C_0 \langle q_L q_R \rangle \\ &\quad + \frac{1}{4} F_{\mu\nu} F_{\mu\nu} + \frac{1}{2} (\partial_\mu A_\mu)^2, \end{aligned} \quad (7)$$

where the superscript (3) labels the number of flavours. Further, $u \cdot u \equiv u_\mu u_\mu$, $F_{\mu\nu} = \partial_\mu A_\nu - \partial_\nu A_\mu$ is the field strength of the photon, and the gauge fixing term is put in the Feynman gauge, as is customary in χ PT_{2,3} ^{γ} . The sym-

bol $\langle \cdot \rangle$ denotes the trace of the flavour matrix enclosed. For two flavours the leading order Lagrangian amounts to having the same form as for three flavours, with the difference of restricting the u fields to elements of $\text{SU}(2)$, and similar for the sources. Furthermore, the LECs F_0 , B_0 , and C_0 are to be replaced with F , B , and C , respectively. To distinguish two- from three-flavour fields, we decorate the former ones with a superscript π . In summary,

$$\begin{aligned} \mathcal{L}_2^{(2)} &= \frac{F^2}{4} \langle u^\pi \cdot u^\pi - \chi_+^\pi \rangle - C \langle q_L^\pi q_R^\pi \rangle \\ &\quad + \frac{1}{4} F_{\mu\nu}^\pi F_{\mu\nu}^\pi + \frac{1}{2} (\partial_\mu A_\mu^\pi)^2. \end{aligned} \quad (8)$$

For the NLO Lagrangian \mathcal{L}_4 we need the following additional building blocks:

$$\begin{aligned} f_{\pm\mu\nu} &= u l_{\mu\nu} u^\dagger \pm u^\dagger r_{\mu\nu} u, \\ \chi_{\pm\mu} &= \nabla_\mu \chi_\pm - \frac{i}{2} \{ \chi_\mp, u_\mu \}, \\ q_{R\mu} &= \nabla_\mu q_R - \frac{i}{2} [u_\mu, q_R], \\ q_{L\mu} &= \nabla_\mu q_L + \frac{i}{2} [u_\mu, q_L], \end{aligned} \quad (9)$$

where we have introduced the field strengths

$$y_{\mu\nu} = \partial_\mu y_\nu - \partial_\nu y_\mu - i [y_\mu, y_\nu], \quad y \in \{r, l\},$$

and the covariant derivative ∇_μ in terms of the chiral connection Γ_μ ,

$$\begin{aligned} \nabla_\mu X &= \partial_\mu X + [\Gamma_\mu, X], \\ \Gamma_\mu &= \frac{1}{2} [u^\dagger (\partial_\mu - i r_\mu) u + u (\partial_\mu - i l_\mu) u^\dagger]. \end{aligned}$$

It is worth noting that $f_{+\mu\nu}$ for two flavours is not traceless, since the charge matrix Q_2 is not. To be in

Table 1. Basis of the strong operators at order p^4 in Euclidean metric for two (x_j) and for three flavours (X_j)

j	x_j	X_j
1	$-\frac{1}{4} \langle u^\pi \cdot u^\pi \rangle^2$	$-\langle u \cdot u \rangle^2$
2	$-\frac{1}{4} \langle u_\mu^\pi u_\nu^\pi \rangle^2$	$-\langle u_\mu u_\nu \rangle^2$
3	$-\frac{1}{16} \langle \chi_+^\pi \rangle^2$	$-\langle (u \cdot u)^2 \rangle$
4	$\frac{i}{4} \langle u_\mu^\pi \chi_-^\pi \rangle$	$\langle u \cdot u \rangle \langle \chi_+ \rangle$
5	$\frac{1}{2} \langle f_-^{\pi 2} \rangle$	$\langle u \cdot u \chi_+ \rangle$
6	$-\frac{i}{4} \langle f_{+\mu\nu}^\pi [u_\mu^\pi, u_\nu^\pi] \rangle$	$-\langle \chi_+ \rangle^2$
7	$\frac{1}{16} \langle \chi_-^\pi \rangle^2$	$-\langle \chi_- \rangle^2$
8	$-\frac{1}{8} (\det \chi_+^\pi + \det \chi_-^\pi)$	$-\frac{1}{2} \langle \chi_+^2 + \chi_-^2 \rangle$
9	$\langle \tilde{f}_+^{\pi 2} + f_-^{\pi 2} \rangle$	$\frac{i}{2} \langle f_{+\mu\nu} [u_\mu, u_\nu] \rangle$
10	$-\frac{1}{16} \langle \chi_+^{\pi 2} - \chi_-^{\pi 2} \rangle$	$-\frac{1}{4} \langle f_+^2 - f_-^2 \rangle$
11	$-\frac{1}{4} \langle f_{+\mu\nu}^\pi \rangle^2$	$-\frac{1}{2} \langle f_+^2 + f_-^2 \rangle$
12		$-\frac{1}{4} \langle \chi_+^2 - \chi_-^2 \rangle$

Table 2. Basis of the electromagnetic operators at order $e^2 p^2$ and e^4 in Euclidean metric for two (w_j) and for three flavours (W_j). The abbreviation $q_A \cdot q_A = q_{A\mu} q_{A\mu}$ for $A \in \{R, L\}$ is adopted

j	w_j	W_j
1	$\frac{1}{2} \langle u^\pi \cdot u^\pi \rangle \langle q_R^\pi{}^2 + q_L^\pi{}^2 \rangle$	$\frac{1}{2} \langle u \cdot u \rangle \langle q_R^2 + q_L^2 \rangle$
2	$\langle u^\pi \cdot u^\pi \rangle \langle q_R^\pi q_L^\pi \rangle$	$\langle u \cdot u \rangle \langle q_R q_L \rangle$
3	$-\langle u_\mu^\pi q_R^\pi \rangle^2 - \langle u_\mu^\pi q_L^\pi \rangle^2$	$-\langle u_\mu q_R \rangle^2 - \langle u_\mu q_L \rangle^2$
4	$\langle u_\mu^\pi q_R^\pi \rangle \langle u_\mu^\pi q_L^\pi \rangle$	$\langle u_\mu q_R \rangle \langle u_\mu q_L \rangle$
5	$-\frac{1}{2} \langle \chi_+^\pi \rangle \langle q_R^\pi{}^2 + q_L^\pi{}^2 \rangle$	$\langle u \cdot u \rangle \langle q_R^2 + q_L^2 \rangle$
6	$-\langle \chi_+^\pi \rangle \langle q_R^\pi q_L^\pi \rangle$	$\langle u \cdot u \rangle \langle q_R q_L \rangle$
7	$-\frac{1}{2} \langle \chi_+^\pi (q_R^\pi + q_L^\pi) \rangle \langle q_R^\pi + q_L^\pi \rangle$	$-\frac{1}{2} \langle \chi_+ \rangle \langle q_R^2 + q_L^2 \rangle$
8	$-\langle \chi_-^\pi [q_R^\pi, q_L^\pi] \rangle$	$-\langle \chi_+ \rangle \langle q_R q_L \rangle$
9	$i \langle u_\mu^\pi \left([q_{R\mu}^\pi, q_R^\pi] - [q_{L\mu}^\pi, q_L^\pi] \right) \rangle$	$-\langle \chi_+ \rangle \langle q_R^2 + q_L^2 \rangle$
10	$\langle q_{R\mu}^\pi q_{L\mu}^\pi \rangle$	$-\langle \chi_+ \rangle \langle q_R q_L \rangle$
11	$\langle q_R^\pi \cdot q_R^\pi + q_L^\pi \cdot q_L^\pi \rangle$	$-\langle \chi_- \rangle \langle q_R q_L \rangle$
12	$-\frac{1}{4} \langle q_R^\pi{}^2 + q_L^\pi{}^2 \rangle^2$	$i \langle u_\mu \rangle \left([q_{R\mu}, q_R] - [q_{L\mu}, q_L] \right)$
13	$-\frac{1}{2} \langle q_R^\pi q_L^\pi \rangle \langle q_R^\pi{}^2 + q_L^\pi{}^2 \rangle$	$\langle q_{R\mu} q_{L\mu} \rangle$
14	$-\langle q_R^\pi q_L^\pi \rangle^2$	$\langle q_R \cdot q_R + q_L \cdot q_L \rangle$
15		$-\langle q_R q_L \rangle^2$
16		$-\frac{1}{2} \langle q_R q_L \rangle \langle q_R^2 + q_L^2 \rangle$
17		$-\frac{1}{4} \langle q_R^2 + q_L^2 \rangle^2$

line with the basis operators introduced by Gasser and Leutwyler [2], it is convenient to introduce in addition the traceless operator $f_{+\mu\nu}^\pi$,

$$\tilde{f}_{+\mu\nu}^\pi = f_{+\mu\nu}^\pi - \frac{1}{2} \langle f_{+\mu\nu}^\pi \rangle. \quad (10)$$

The NLO Lagrangians \mathcal{L}_4 then read

$$\mathcal{L}_4^{(2)} = \sum_{j=1}^{11} l_j x_j + F^2 \sum_{j=1}^{11} k_j w_j + F^4 \sum_{j=12}^{14} k_j w_j, \quad (11)$$

$$\mathcal{L}_4^{(3)} = \sum_{j=1}^{12} L_j X_j + F_0^2 \sum_{j=1}^{14} K_j W_j + F_0^4 \sum_{j=15}^{17} K_j W_j. \quad (12)$$

In the following, we call the operators x_j , X_j and the LECs l_j , L_j *strong operators* and *strong LECs*, as these operators do not vanish when switching off the electromagnetic coupling constant, with the exception of x_{11} . Accordingly, we denote the operators/LECs w_j , W_j/k_j , K_j *electromagnetic operators/LECs*. The strong operators x_j and X_j have been introduced by Gasser and Leutwyler [2, 3] and, for convenience, we reproduce them here in Table 1. The coefficients h_i and H_i of the contact terms – introduced by Gasser and Leutwyler in [2, 3] – are related to our LECs by

$$\begin{aligned} h_1 - h_3 &= l_8, & h_2 &= l_9, & h_1 + h_3 &= l_{10}, \\ H_1 &= L_{11}, & H_2 &= L_{12}. \end{aligned} \quad (13)$$

We are using the set of the NLO electromagnetic operators from Knecht and Urech [9] for two, and from Urech [6] for three flavours; see Table 2. We do not consider the odd-intrinsic parity sector, which accounts for the axial anomaly; see e.g. [28–31]. For the counting we rely on the standard χ PT $^\gamma$ assignment with $e^2 \sim O(p^2)$ and we make use of the convention of writing $O(e^4, e^2 p^2, p^4)$ as $O(p^4)$, and similarly for the Landau symbol at order p^6 .

3 Integrating out the strange quark

This section is devoted to give some details on the derivation of the main results presented below in (42). We will follow the steps outlined in [21, 22].

3.1 Generating functional

We start by considering the generating functional Z of χ PT $_3^\gamma$ [3],

$$e^{-Z[v, a, s, p, Q_L, R]} = \mathcal{N} \int [du][dA_\mu] e^{-\int d^d x \mathcal{L}_{\text{eff}}^{(3)}}, \quad (14)$$

$$\mathcal{L}_{\text{eff}}^{(3)} = \mathcal{L}_2^{(3)} + \mathcal{L}_4^{(3)} + \dots \quad (15)$$

It may be evaluated in a low-energy expansion in the number of loops,

$$Z = Z_0 + Z_1 + \dots, \quad (16)$$

where Z_0 (Z_1) collects the tree-level (one-loop) contributions. They are given by

$$Z_0 = \bar{S}_2, \quad (17)$$

$$Z_1 = \bar{S}_4 + \frac{1}{2} \ln \frac{\det D}{\det D^0}, \quad (18)$$

where \bar{S}_n denotes the classical action

$$\bar{S}_n = \int d^d x \mathcal{L}_n^{(3)}(u^{\text{cl}}, A^{\text{cl}}, v, a, s, p, Q_{L,R}), \quad (19)$$

the Goldstone boson fields u^{cl} and the photon field A_μ^{cl} being evaluated at the solution of the classical equation of motion (EOM),

$$\nabla_\mu u_\mu^{\text{cl}} + \frac{i}{2} \tilde{\chi}^{\text{cl}} + 2i \frac{C_0}{F_0^2} [q_R^{\text{cl}}, q_L^{\text{cl}}] = 0, \quad (20)$$

$$\Delta A_\mu^{\text{cl}} - \frac{F_0^2}{2} \langle u_\mu^{\text{cl}} (q_R^{\text{cl}} - q_L^{\text{cl}}) \rangle = 0, \quad (21)$$

where $\tilde{\chi}^{\text{cl}}$ denotes the traceless part of χ^{cl} . The Green's function of the differential operator D [D^0] of (18) is the [free] propagator $G(x, y)$, [$G_0(x, y)$],

$$D_{AC}(x) G_{CB}(x, y) = \delta_{AB} \delta^{(d)}(x - y). \quad (22)$$

The explicit form of D was first given by Urech [6]²,

$$D(x) = -\Sigma^2(x) + \Lambda(x), \quad \Sigma_\mu(x) = \partial_\mu^x + Y_\mu(x), \quad (23)$$

with³

$$\begin{aligned} Y_\mu &= \begin{pmatrix} \hat{\Gamma}_\mu^{ab} & X_\mu^{a\rho} \\ X_\mu^{\sigma b} & 0 \end{pmatrix}, \quad \Lambda = \begin{pmatrix} \sigma^{ab} & \frac{1}{2} \gamma^{a\rho} \\ \frac{1}{2} \gamma^{\sigma b} & \rho \delta^{\sigma\rho} \end{pmatrix}, \\ \hat{\Gamma}_\mu^{ab} &= -\frac{1}{2} \langle [\lambda^a, \lambda^b] \Gamma_\mu \rangle, \\ X_\mu^{a\rho} &= -X_\mu^{\rho a} = -\frac{F_0}{4} \delta_\mu^\rho \langle \lambda^a (q_R - q_L) \rangle, \\ \sigma^{ab} &= \frac{1}{8} \langle [\lambda^a, u_\mu] [\lambda^b, u_\mu] \rangle + \frac{1}{8} \langle \{ \lambda^a, \lambda^b \} \chi_+ \rangle \\ &\quad - \frac{C_0}{4F_0^2} \langle ([\lambda^a, q_R + q_L] [\lambda^b, q_R + q_L] \\ &\quad - [\lambda^a, q_R - q_L] [\lambda^b, q_R - q_L]) \rangle \\ &\quad - \frac{F_0^2}{4} \langle \lambda^a (q_R - q_L) \rangle \langle \lambda^b (q_R - q_L) \rangle, \\ \gamma_\mu^a &= \frac{F_0}{2} \langle \lambda^a \{ \nabla_\mu (q_R - q_L) + i [u_\mu, q_R + q_L] \} \rangle, \\ \rho &= \frac{3}{8} F_0^2 \langle (q_R - q_L)^2 \rangle. \end{aligned} \quad (24)$$

² Capital flavour indices A, B, C, \dots run from 1 to 12, lower case flavour indices from 1 to 8; they span the meson flavour space. Greek indices ρ, σ, \dots run from 1 to 4 for the photon field components. The symbols λ^a stand for the Gell-Mann matrices.

³ For easy reading, we will drop from now on the label cl for the fields that satisfy the EOM.

The generating functional for two flavours z is defined analogously to the one with three flavours. For later purposes we explicitly introduce its low-energy expansion up to one loop,

$$z = \bar{s}_2 + \bar{s}_4 + \frac{1}{2} \ln \frac{\det d}{\det d^0} + \dots, \quad (25)$$

where $\bar{s}_{2,4}$ and the operator d are the two-flavour equivalent of (19) and (23), and the ellipsis stands for two-loop corrections and higher. For a state-of-the-art evaluation of the two-flavour functional and more details we refer the reader to Schweizer [32].

3.2 Matching

We now impose the following constraints on the three-flavour functional:

- i) the external sources of χPT_3^γ are restricted to the two-flavour subspace. The generating functionals shall depend on the *same* external sources;
- ii) $m_{u,d} \ll m_s$; since the LECs of $\chi\text{PT}_{2,3}^\gamma$ are independent of $m_{u,d}$, we will work in the chiral limit for the up and down quark masses, i.e. $m_{u,d} = 0$, for simplicity;
- iii) external momenta are restricted to values below the threshold of the massive fields, $|p^2| \ll M_K^2$.

We will refer to the limit that satisfies i), ii) and iii) as *the two-flavour limit* of the three-flavour theory. In this limit the three-flavour functional reduces to the two-flavour functional, i.e. both theories yield the same Green's functions in the low-energy region,

$$Z = z, \quad (26)$$

provided the LECs of both theories are accordingly matched. In the following, we will solve this equation for the LECs. Both sides receive non-local contributions that are associated to the propagation of massless pions and photons. Once the matching is fully worked out, these contributions cancel each other. At order p^4 , this has been discussed in detail by Nyffeler and Schenk [21] and further details will also be given elsewhere [33]. To find the relations among the LECs it suffices therefore to work out the *local* parts of the generating functionals. At order p^4 we have in the two-flavour limit

$$\bar{S}_2 + \bar{S}_4 + \frac{1}{2} \ln \frac{\det D}{\det D^0} \Big|_{\text{local}} = \bar{s}_2 + \bar{s}_4. \quad (27)$$

The l.h.s. of (27) is now being worked out. We start with the tree-level contributions and proceed with the one-loop corrections.

3.2.1 Tree level: solution of the EOM in the two-flavour limit

In view of (17) and (18) we need to solve the EOM in the two-flavour limit. Due to the absence of strangeness containing external sources [restriction i)] as well as

strangeness conservation, the following ansatz for the Goldstone boson fields will turn out to be fruitful:

$$u = u^\pi e^{\frac{i}{2F_0} \eta \lambda^8}, \quad (28)$$

where in u^π only the pions contribute non-trivially. Below, we will frequently identify without further notice 3×3 matrices that have only non-vanishing elements in their upper left 2×2 block with the 2×2 matrices from the two-flavour theory. Inserting the ansatz (28) into the building blocks (3) yields

$$\begin{aligned} u_\mu &= u_\mu^\pi - \frac{1}{F_0} \lambda^8 \partial_\mu \eta, \\ q_{L,R} &= q_{L,R}^\pi - e_{33} \langle q_{L,R}^\pi \rangle, \\ \chi_\pm &= \frac{B_0}{B} \chi_\pm^\pi \cos \alpha - i \frac{B_0}{B} \chi_\mp^\pi \sin \alpha \\ &\quad + 4B_0 m_s e_{33} \begin{cases} \cos 2\alpha & (+), \\ i \sin 2\alpha & (-), \end{cases} \end{aligned} \quad (29)$$

$$\alpha = \eta / (\sqrt{3} F_0), \quad e_{33} = \text{diag}(0, 0, 1). \quad (30)$$

And similar for the building blocks of (9),

$$\begin{aligned} f_{+\mu\nu} &= f_{+\mu\nu}^\pi - e_{33} \langle f_{+\mu\nu}^\pi \rangle, \quad f_{-\mu\nu} = f_{-\mu\nu}^\pi, \\ q_{A\mu} &= q_{A\mu}^\pi, \quad A \in \{R, L\}. \end{aligned} \quad (31)$$

Next, we write down the EOM of the η field,

$$\begin{aligned} (\Delta - M_\eta^2) \eta &= \frac{F_0}{4\sqrt{3}} \left[\frac{B_0}{B} \langle \chi_+^\pi \rangle \sin \alpha + i \frac{B_0}{B} \langle \chi_-^\pi \rangle \cos \alpha \right. \\ &\quad \left. + 8B_0 m_s \sin 2\alpha \right] - M_\eta^2 \eta, \end{aligned} \quad (32)$$

where $M_\eta^2 = \frac{4}{3} B_0 m_s$ is the eta mass squared at tree level at $m_{u,d} = 0$ [similarly we will use $M_K^2 = B_0 m_s$ below]. The EOM may be solved recursively for small α . Note that the sum of the last two terms in (32) is of order α^3 . The differential equation suggests a counting in which every occurrence of an η particle counts as order p^2 in the two-flavour limit,

$$\eta = -\frac{i\sqrt{3}F_0}{16Bm_s} \langle \chi_-^\pi \rangle + O(p^4). \quad (33)$$

As a result, we obtain a systematic low-energy expansion of the SU(3) building blocks.

Before proceeding, we add a remark: to be precise, the pions of χ PT₃^γ differ from their two-flavour equivalent, since they satisfy different EOMs. Indeed, in the two-flavour limit, we find

$$\nabla_\mu u_\mu^\pi + \frac{i}{2} \frac{B_0}{B} \tilde{\chi}_-^\pi \cos \alpha + \frac{1}{2} \frac{B_0}{B} \tilde{\chi}_+^\pi \sin \alpha + 2i \frac{C_0}{F_0^2} [q_R^\pi, q_L^\pi] = 0, \quad (34)$$

to be compared with the EOM of χ PT₂^γ,

$$\nabla_\mu u_\mu^\pi + \frac{i}{2} \tilde{\chi}_-^\pi + 2i \frac{C}{F^2} [q_R^\pi, q_L^\pi] = 0. \quad (35)$$

However, expanding the trigonometric functions in (34), one observes that the difference is of order p^4 ; hence, it affects the matching relations only beyond the accuracy at which we are working. Also at the level of \bar{S}_2 – which is the only one to matter for the EOM – the LECs of both theories coincide due to the matching condition (26). These are the reasons why we do not distinguish between the pions of both theories in this article. However, if one wishes to carry out the matching beyond one-loop order, this issue requires a considerably deeper examination [33]. Similar remarks apply for the photon.

By now, it is straightforward to evaluate the tree-level diagrams of $\bar{S}_{2,4}$ in the two-flavour limit using (29), (31) and (33). To avoid overflowing formulae, for \bar{S}_4 we only show the reduction of the electromagnetic operators explicitly. We find

$$\begin{aligned} \bar{S}_2 &= \int d^d x \left[\frac{F_0^2}{4} \langle u^\pi \cdot u^\pi \rangle - \frac{F_0^2}{4} (B_0/B) \langle \chi_+^\pi \rangle - C_0 \langle q_L^\pi q_R^\pi \rangle \right. \\ &\quad \left. + \frac{1}{4} F_{\mu\nu}^\pi F_{\mu\nu}^\pi + \frac{1}{2} (\partial_\mu A_\mu^\pi)^2 + \frac{F_0^2}{8M_K^2} (B_0/B)^2 x_7 \right] + O(p^6), \\ \bar{S}_4 &= F_0^2 \int d^d x \left\{ -4M_K^2 K_8 \langle q_L^\pi q_R^\pi \rangle \right. \\ &\quad + \left(\frac{6}{5} K_1 + \frac{1}{5} K_2 + K_5 \right) w_1 + (K_2 + K_6) w_2 + K_3 w_3 \\ &\quad + K_4 w_4 + \left(\frac{6}{5} K_7 + \frac{1}{5} K_8 + \frac{4}{5} K_9 - \frac{1}{5} K_{10} \right) w_5 \\ &\quad + (K_8 + K_{10}) w_6 + (K_9 + K_{10}) w_7 + K_{11} w_8 + K_{12} w_9 \\ &\quad + K_{13} w_{10} + K_{14} w_{11} \\ &\quad + F_0^2 \left[\left(\frac{1}{25} K_{15} + \frac{6}{25} K_{16} + \frac{36}{25} K_{17} \right) w_{12} \right. \\ &\quad \left. + \left(\frac{2}{5} K_{15} + \frac{6}{5} K_{16} \right) w_{13} + K_{15} w_{14} \right] \left. \right\} \\ &\quad + \bar{S}_4|_{\text{strong}} + O(p^6). \end{aligned} \quad (36)$$

3.2.2 Loops: the determinant in the two-flavour limit

The determinant of the differential operator D covers all one-loop diagrams of the generating functional. Its evaluation in terms of an expansion in external fields in the two-flavour limit may be worked out as follows. To begin with, we note that the contributions from the massless (pions and photon) and from the massive fields (kaons and eta) may be separated [21, 22],

$$\begin{aligned} \ln \det D &= \ln \det D_\ell + \ln \det D_\eta + \ln \det D_K \\ &\quad + \ln \det (1 - D_\pi^{-1} D_{\pi\eta} D_\eta^{-1} D_{\eta\pi}). \end{aligned} \quad (37)$$

The first determinant $\ln \det D_\ell$ involves contributions from pions and photons only; it is a purely non-local object and for the matching of the LECs needs not to be considered any further. The operators D_η and D_K are related to heavy particles only: their determinants describe tadpoles with insertions where only particles of identical masses run in the loop, either etas or kaons; cf. Fig. 1 (left).

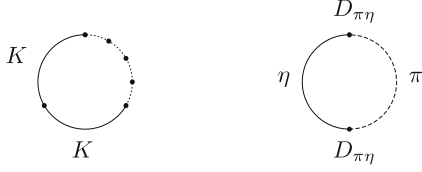


Fig. 1. (Left:) diagrammatic illustration for a specific contribution to $\ln \det D_K$ in (37). The vertices denote insertions from external fields, related to the operator D . Only kaons flow through the loop. The whole determinant consists of a sum of such diagrams, ordered by an increasing number of insertions, being equivalent to the low-energy expansion introduced in the text. (Right:) pion-eta mixing at order p^4 . In the two-flavour limit this diagram yields local terms only

Diagrams of this type are efficiently calculated with heat-kernel methods. It results in an expansion in terms of local quantities involving an increasing number of derivatives, which corresponds to an expansion in powers of momenta. The last determinant on the r.h.s. of (37) is a more complicated object. Since it involves the operator D_π of the massless modes, it is not a purely local object. However, its non-locality in the low-energy expansion only shows up at order p^6 and can therefore be neglected for our analysis. This is due to the symmetric operator $D_{\pi\eta}$, which mediates π - η mixing and is of order p^2 . At order p^4 , the operators D_π^{-1} and D_η^{-1} may be replaced by their free propagators. As a result, the diagram of Fig. 1 (right) is the only contribution from the last term in (37) at order p^4 . And the low-energy expansion of this diagram yields local terms only. The photon does not show up in this mixing term, because the eta is not charged. We find

$$\begin{aligned} & \frac{1}{2} \ln(\det D / \det D^0)|_{\text{local}} \\ &= \int d^d x \left(\mathcal{L}_{1\text{loop}}^\eta + \mathcal{L}_{1\text{loop}}^K + \mathcal{L}_{1\text{loop}}^{\pi\eta} \right) + O(p^6), \\ \mathcal{L}_{1\text{loop}}^\eta &= \frac{1}{24} F_1(M_\eta^2) \left[\langle \chi_+^\pi \rangle + M_K^{-2} x_7 \right] + \frac{1}{36} F_2(M_\eta^2) x_3, \\ \mathcal{L}_{1\text{loop}}^K &= -\frac{1}{4} F_1(M_K^2) \left[\langle u_\mu^\pi u_\mu^\pi - \chi_+^\pi \rangle - 8 \frac{C_0}{F_0^2} \langle q_R^\pi q_L^\pi \rangle \right] \\ &+ \frac{1}{48} F_2(M_K^2) \left(x_1 + 2x_2 + 12x_4 - 2x_5 - 4x_6 \right. \\ &- 12x_7 + x_9 + 24x_{10} - 18x_{11} \\ &+ \frac{C_0}{F_0^2} \left[\frac{48}{5} w_1 + 12w_2 + \frac{12}{5} w_5 + 12w_6 + 36w_7 \right. \\ &\left. \left. - 6w_8 + \frac{C_0}{F_0^2} \left(\frac{2496}{25} w_{12} + \frac{816}{5} w_{13} + 48w_{14} \right) \right] \right), \\ \mathcal{L}_{1\text{loop}}^{\pi\eta} &= -\frac{1}{6} F_2^1(M_\eta^2) (x_7 + x_8 - x_{10}), \end{aligned} \quad (38)$$

where the $F_n^l(m^2)$ denote loop integrals,

$$\begin{aligned} F_n^l(m^2) &= \int \frac{d^d q}{(2\pi)^d} \frac{1}{(m^2 + q^2)^{n-l} (q^2)^l}, \quad n > l \geq 0, \\ F_n(m^2) &\equiv F_n^0(m^2), \end{aligned} \quad (40)$$

which are well known, cf. e.g. [34]. The renormalisation is carried out in the $\overline{\text{MS}}$ -scheme, where the LECs $c_i \in \{l_i, k_i, L_i, K_i\}$ are split into a divergent and a finite part, as follows:

$$\begin{aligned} c_i &= \alpha_i \lambda + c_i^r(\mu, d), \quad c_i^r(\mu) \equiv c_i^r(\mu, 4), \\ \lambda &= \frac{\mu^{d-4}}{16\pi^2} \left\{ \frac{1}{d-4} - \frac{1}{2} [\ln 4\pi + \Gamma'(1) + 1] \right\}. \end{aligned} \quad (41)$$

The coefficients $\alpha_i \in \{\gamma_i, \sigma_i, \Gamma_i, \Sigma_i\}$ are given in [2, 3, 6, 9].⁴

3.3 Results

Collecting the results of the tree (36) and one-loop (39) analysis allows us to determine the relationship among the three- and two-flavour LECs via (27). The results are

$$\begin{aligned} C &= C_0 [1 - 4\mu_K] + 4M_K^2 F_0^2 K_8^r, \\ k_1^r &= \frac{6}{5} K_1^r + \frac{1}{5} K_2^r + K_5^r - \frac{2}{5} Z_0 \nu_K, \\ k_2^r &= K_2^r + K_6^r - \frac{1}{2} Z_0 \nu_K, \\ k_3^r &= K_3^r, \\ k_4^r &= K_4^r, \\ k_5^r &= \frac{6}{5} K_7^r + \frac{1}{5} K_8^r + \frac{4}{5} K_9^r - \frac{1}{5} K_{10}^r - \frac{1}{10} Z_0 \nu_K, \\ k_6^r &= K_8^r + K_{10}^r - \frac{1}{2} Z_0 \nu_K, \\ k_7^r &= K_9^r + K_{10}^r - \frac{3}{2} Z_0 \nu_K, \\ k_8^r &= K_{11}^r - 2Z_0(2L_4^r + L_5^r) + \frac{1}{4} Z_0 \nu_K, \\ k_9^r &= K_{12}^r, \\ k_{10}^r &= K_{13}^r, \\ k_{11}^r &= K_{14}^r, \\ k_{12}^r &= \frac{1}{25} K_{15}^r + \frac{6}{25} K_{16}^r + \frac{36}{25} K_{17}^r - \frac{104}{25} Z_0^2 \nu_K, \\ k_{13}^r &= \frac{2}{5} K_{15}^r + \frac{6}{5} K_{16}^r - \frac{34}{5} Z_0^2 \nu_K, \\ k_{14}^r &= K_{15}^r - 2Z_0^2 \nu_K, \\ l_{11} &= \frac{3}{2} L_{10}^r + 3L_{11}^r + \frac{3}{4} \nu_K, \end{aligned} \quad (42)$$

where we introduced the abbreviations

$$\begin{aligned} Z_0 &= C_0/F_0^4, \quad \mu_K = \frac{M_K^2}{32\pi^2 F_0^2} \ln \frac{M_K^2}{\mu^2}, \\ \nu_K &= \frac{1}{32\pi^2} \left(\ln \frac{M_K^2}{\mu^2} + 1 \right). \end{aligned} \quad (43)$$

These relations are the main results of our article and deserve a few comments.

- We only display the matching relations for the electromagnetic LECs as well as the strong LEC l_{11} . The

⁴ For $\Sigma_{15,16,17}$ consult (12) in [10].

ones for the remaining strong LECs may be established along the very same lines and may be found in [3, 23].

- At first glance it might come as a surprise that strong three-flavour LECs show up in the matching of the electromagnetic LECs, cf. k_8^r . Along the derivation presented here it is the EOM that links strong and electromagnetic operators and needs to be used to project the operators X_4 and X_5 (in the two-flavour limit) into the two-flavour basis.
- Briefly, we go back again to (39). We remark that only the kaon loop contributes non-trivially to the matching of the electromagnetic LECs. Having in mind that along the method presented here, we had performed the matching for the strong LECs l_i at two loops already before [23, 33], the relations in (42) come at almost no additional cost. Exactly here lies the beauty of this approach: once the framework is set, all relations of the LECs are obtained in one strike at a reasonable amount of effort.
- One verifies that the dependence on the scale μ of the left and right hand side of (42) is the same.
- Specific linear combinations for electromagnetic matching relations were presented earlier in [18]. We completely agree with the relations given there. Some of the relations were also given in [19, 20]; see [35] for comments on why some of the relations in [19] were given erroneously.
- The approach that was advocated in [18, 19, 24] relied on an analysis of physical observables – e.g. the charged pion mass or $\pi\pi$ -scattering – both in χ PT $_3^\gamma$ as well as in χ PT $_2^\gamma$. The functional relationship among (linear combinations of) the LECs emerges then from a comparison of the two representations in a large m_s expansion. The agreement between the results found in the literature and those presented here based on the generating functional provides a thorough and welcome check on both calculations.

4 Numerical analysis

The relations derived in (42) are useful to obtain constraints on the pertinent LECs. In the strong sector for instance, already in the early days of χ PT Gasser and Leutwyler made use of such relations to convert information about the values of the two-flavour LECs to determine three-flavour LECs; e.g. an estimate for L_2 was obtained in this way via l_2 . The formulae here presented may be used in an analogous fashion: to the best of our knowledge only estimates for the LECs in χ PT $_3^\gamma$ are known [12–17]. The matching relations may thus be inferred to obtain estimates on the values of the two-flavour coupling constants. Two remarks should be made that are relevant in the numerical determination of the LECs: first, some of the LECs depend on the gauge [15, 36]. The values inferred below are evaluated in the Feynman gauge. Second, due to ultraviolet divergences generated by photon loops, the splitting of the Hamiltonian of QCD + γ into a strong and an elec-

tromagnetic piece is ambiguous. This ambiguity must be reflected also in the effective theory in the LECs [37]. Estimates of their sizes should therefore take this into account. The authors of [37] have discussed the problem in detail on the basis of field theoretic models and have come up with a proposal on how the ambiguity may be addressed systematically within these models. Still, this delicate issue has not been investigated in the literature for the χ PT $_{2,3}^\gamma$ LECs yet and is beyond the scope of what we are aiming at here.

We proceed with the numerical analysis of (42). At the accuracy we are working, we may identify F_0 with the pion decay constant $F_\pi = 92.4$ MeV and $M_K^2 = B_0 m_s$ with

$$B_0 m_s = M_{K^+}^2 - M_{\pi^+}^2 / 2 \simeq (485 \text{ MeV})^2. \quad (44)$$

We further set $Z_0 = 0.91$ (obtained from (42) of [15] with $M_V = 0.77$ GeV, $z \equiv M_A^2 / M_V^2 = 2$). For the values of the three-flavour NLO electromagnetic LECs for K_1^r, \dots, K_6^r we will stick to [12], and for K_7, \dots, K_{12}^r to [15], summarised here in Table 3. The LEC K_9^r remained undetermined in [15], as it yet suffers from a reliable estimate [15]. As a result we will not give a numerical estimate for k_5^r and k_7 . For the LECs K_{11}^r and K_{12}^r (from (59) and (61) in [15]) we furthermore set $\mu_0 = 1$ GeV for the QCD scale, and the parameters M_V and z are as introduced above. The coupling constants $K_{14}^r, \dots, K_{17}^r$ are associated to contact operators and/or operators at order e^4 and are not considered in this section. Furthermore, $L_4^r = 0$ and $L_5^r = 1.5 \times 10^{-3}$, taken from the $O(p^4)$ fit in [38]. All LECs are evaluated at the scale $\mu = 0.77$ GeV, and in the Feynman gauge, $\xi = 1$. The results for the electromagnetic two-flavour LECs so obtained are finally summarised in Table 4. As an illustration we also show in Fig. 2 the strange quark mass dependence of k_1^r and k_2^r . We observe that the two-flavour LECs only show a very moderate strange quark mass dependence in the neighbourhood of the physical point. This pattern is due to its solely logarithmic strange quark mass dependence at this order of the matching. Note that the matching relations only apply over a certain range for the strange quark mass: the formulae break down for $m_s \rightarrow 0$, as the expansion performed here requires that all exter-

Table 3. Values of electromagnetic LECs in χ PT $_3^\gamma$ in units of 10^{-3} at the scale $\mu = M_\rho = 0.77$ GeV, in the Feynman gauge. The values for K_1^r, \dots, K_6^r are invoked from [12], and K_7, \dots, K_{13} from [15]; see also the text for further details

K_1^r	−2.7	K_7	0
K_2^r	0.7	K_8^r	0
K_3^r	2.7	K_9^r	−
K_4^r	1.4	K_{10}^r	4.0
K_5^r	11.6	K_{11}^r	1.3
K_6^r	2.8	K_{12}^r	−4.2
		K_{13}	4.7

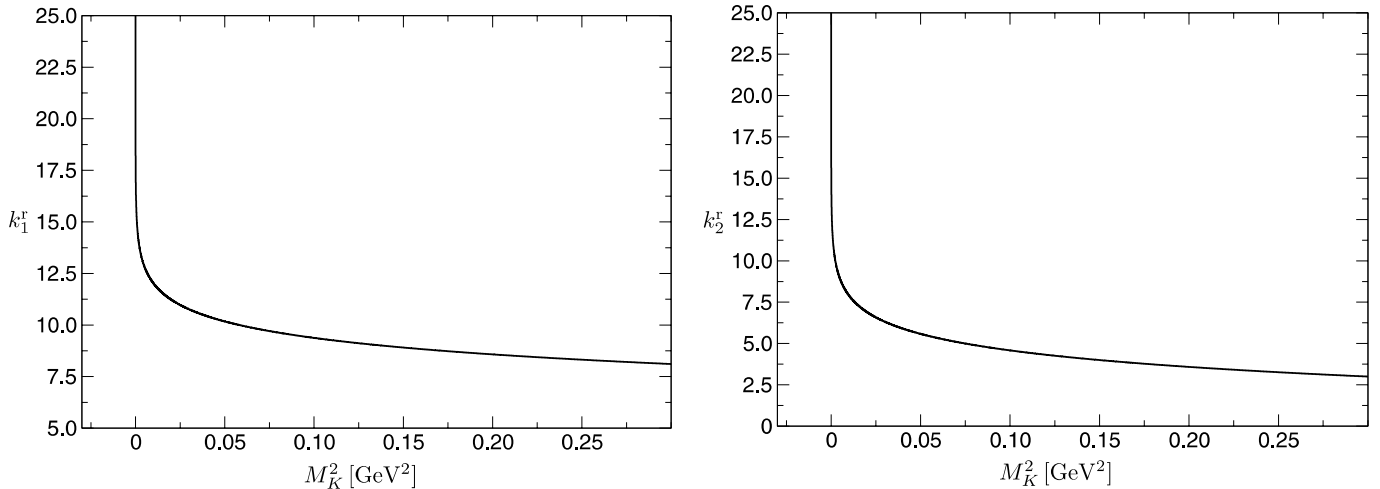


Fig. 2. Strange quark mass dependence of the electromagnetic two-flavour LECs k_1^r (left) and k_2^r (right) in units of 10^{-3} at the scale $\mu = M_\rho = 0.77$ GeV. The physical value of m_s corresponds to $M_K^2 = B_0 m_s \approx (485 \text{ MeV})^2$

Table 4. Values of electromagnetic low-energy constants in χPT_2^γ in units of 10^{-3} at the scale $\mu = M_\rho = 0.77$ GeV, in the Feynman gauge. From general dimensional arguments, one might attribute an uncertainty of $1/(16\pi^2) \approx 6.3 \times 10^{-3}$ to each LEC

k_1^r	8.4	k_6^r	3.9
k_2^r	3.4	k_7	$3.7 + K_9^r \cdot 10^3$
k_3^r	2.7	k_8^r	-1.4
k_4^r	1.4	k_9^r	-4.2
k_5^r	$-0.8 + 4/5 K_9^r \cdot 10^3$	k_{10}	4.7

nal momenta are much smaller than m_s . Remarkably, the pertinent chiral logarithm becomes dominant numerically only for very small m_s . On the other hand, as one increases the strange quark mass, higher order contributions in the matching expansion become more dominant and start to spoil the behaviour of the chiral logarithm. This was discussed in more detail in [23] for the strong LECs l_i .

We consider it difficult to assign reliable errors to the estimates of the LECs in Table 4. The determinations in [12, 13, 15] – from which we invoked the K_i^r – are model dependent, for which reliable estimates of uncertainties are always a delicate affair. Moreover, the scale dependence in various LECs can be strongly correlated. We shall therefore refrain from assigning individual errors to the estimates in Table 4. To be conservative, one might attribute an uncertainty of $1/(16\pi^2) \approx 6.3 \times 10^{-3}$ to each LEC k_i^r , stemming from general dimensional arguments. The size of this uncertainty compared to the values in Table 4 indicates that the entries of the table are yet only a rough order of magnitude estimate.

In the near future, a more precise determination of (some combinations of) electromagnetic LECs may also be expected from lattice QCD. In this respect we mention two recent studies that address the electromagnetic splitting of the pseudoscalar meson masses [39, 40].

5 Conclusions

In summary, we have worked out the strange quark mass dependence of the two-flavour electromagnetic LECs, C and k_i , at next-to-leading order. The calculation relied on a non-trivial matching between the three-flavour and the two-flavour generating functional of χ PT including virtual photons and it amounts to 16 relations among the LECs of χPT_2^γ and χPT_3^γ .

These relations are useful to obtain constraints and further information on the pertinent LECs. As an application we have used these relations to obtain numerical estimates for the values of the two-flavour electromagnetic LECs.

Acknowledgements. We thank Jürg Gasser for suggesting us to undertake this work, and we are grateful for many enlightening discussions and comments on the manuscript. We further thank Marc Knecht, Bachir Moussallam and Hagop Satzjian for useful discussions and/or comments on the manuscript. C.H. and M.A.I. wish to express their gratitude to the members of the Institute of Theoretical Physics, University of Bern, for their kind hospitality during the final stages of this work. This work was supported by the Swiss National Science Foundation, by the Ministerio de Educación y Ciencia under the project FPA2004-00996, by Generalitat Valenciana GVACOMP2007-156, and by EU MRTN-CT-2006-035482 (FLAVIA net).

References

1. S. Weinberg, *Physica A* **96**, 327 (1979)
2. J. Gasser, H. Leutwyler, *Ann. Phys.* **158**, 142 (1984)
3. J. Gasser, H. Leutwyler, *Nucl. Phys. B* **250**, 465 (1985)
4. G. Ecker, hep-ph/0702263
5. J. Bijnens, arXiv:0708.1377 [hep-lat]
6. R. Urech, *Nucl. Phys. B* **433**, 234 (1995) [hep-ph/9405341]
7. H. Neufeld, H. Rupertsberger, *Z. Phys. C* **71**, 131 (1996) [hep-ph/9506448]
8. H. Neufeld, H. Rupertsberger, *Z. Phys. C* **68**, 91 (1995)

9. M. Knecht, R. Urech, Nucl. Phys. B **519**, 329 (1998) [hep-ph/9709348]
10. U.G. Meissner, G. Muller, S. Steininger, Phys. Lett. B **406**, 154 (1997) [hep-ph/9704377]
11. U.G. Meissner, G. Muller, S. Steininger, Phys. Lett. B **407**, 454 (1997) [Erratum]
12. B. Ananthanarayan, B. Moussallam, JHEP **0406**, 047 (2004) [hep-ph/0405206]
13. R. Baur, R. Urech, Nucl. Phys. B **499**, 319 (1997) [hep-ph/9612328]
14. J. Bijnens, J. Prades, Nucl. Phys. B **490**, 239 (1997) [hep-ph/9610360]
15. B. Moussallam, Nucl. Phys. B **504**, 381 (1997) [hep-ph/9701400]
16. V.E. Lyubovitskij, T. Gutsche, A. Faessler, R. Vinh Mau, Phys. Lett. B **520**, 204 (2001) [hep-ph/0108134]
17. V.E. Lyubovitskij, T. Gutsche, A. Faessler, R. Vinh Mau, Phys. Rev. C **65**, 025 202 (2002) [hep-ph/0109213]
18. J. Gasser, V.E. Lyubovitskij, A. Rusetsky, A. Gall, Phys. Rev. D **64**, 016 008 (2001) [hep-ph/0103157]
19. H. Jallouli, H. Sazdjian, Phys. Rev. D **58**, 014 011 (1998) [hep-ph/9706450]
20. H. Jallouli, H. Sazdjian, Phys. Rev. D **58**, 099 901 (1998) [Erratum]
21. A. Nyffeler, A. Schenk, Ann. Phys. **241**, 301 (1995) [hep-ph/9409436]
22. M. Schmid, Strangeless χ PT at large m_s , PhD thesis (University of Bern, 2007)
23. J. Gasser, C. Haefeli, M.A. Ivanov, M. Schmid, Phys. Lett. B **652**, 21 (2007) arXiv:0706.0955 [hep-ph]
24. A. Nehme, La Brisure d'Isospin dans les Interactions Méson-Méson à Basse Energie, PhD thesis (CPT Marseille, 2002)
25. B. Moussallam, JHEP **0008**, 005 (2000) [hep-ph/0005245]
26. R. Kaiser, J. Schweizer, JHEP **0606**, 009 (2006) [hep-ph/0603153]
27. M. Frink, U.G. Meissner, JHEP **0407**, 028 (2004) [hep-lat/0404018]
28. J. Wess, B. Zumino, Phys. Lett. B **37**, 95 (1971)
29. E. Witten, Nucl. Phys. B **223**, 422 (1983)
30. R. Kaiser, Phys. Rev. D **63**, 76 010 (2001) [hep-ph/0011377]
31. B. Ananthanarayan, B. Moussallam, JHEP **0205**, 052 (2002) [hep-ph/0205232]
32. J. Schweizer, JHEP **0302**, 007 (2003) [hep-ph/0212188]
33. J. Gasser, C. Haefeli, M.A. Ivanov, M. Schmid, in preparation
34. J. Gasser, M.E. Sainio, Eur. Phys. J. C **6**, 297 (1999) [hep-ph/9803251]
35. H. Sazdjian, Phys. Lett. B **490**, 203 (2000) [hep-ph/0004226]
36. J. Bijnens, Phys. Lett. B **306**, 343 (1993) [hep-ph/9302217]
37. J. Gasser, A. Rusetsky, I. Scimemi, Eur. Phys. J. C **32**, 97 (2003) [hep-ph/0305260]
38. G. Amoros, J. Bijnens, P. Talavera, Nucl. Phys. B **602**, 87 (2001) [hep-ph/0101127]
39. T. Blum, T. Doi, M. Hayakawa, T. Izubuchi, N. Yamada, arXiv:0708.0484 [hep-lat]
40. JLQCD Collaboration, E. Shintani, H. Fukaya, S. Hashimoto, H. Matsufuru, J. Noaki, T. Onogi, N. Yamada, arXiv:0710.0691 [hep-lat]